Copyright WILEY-VCH Verlag GmbH & Co. KGaA, 69469 Weinheim, Germany, 2013.

ADVANCED FUNCTIONAL MATERIALS

Supporting Information

for *Adv. Funct. Mater.*, DOI: 10.1002/adfm.201301913

Domain Wall Displacement is the Origin of Superior Permittivity and Piezoelectricity in $BaTiO_3$ at Intermediate Grain Sizes

*Dipankar Ghosh , Akito Sakata, Jared Carter, Pam A. Thomas , Hyuksu Han, Juan C. Nino , and Jacob L. Jones **

Submitted to ADVANCED FUNCTIONAL MATERIALS

Supporting Information

for Adv. Funct. Mater., DOI: 10.1002/adfm.201301913

Domain Wall Displacement is the Origin of Superior Permittivity and Piezoelectricity in $BaTiO_3$ at Intermediate Grain Sizes

*Dipankar Ghosh, Akito Sakata, Jared Carter, Pam A. Thomas, Hyuksu Han, Juan C. Nino and Jacob L. Jones**

Procedures and Materials

Materials synthesis

For samples sintered via spark plasma sintering (SPS), 5 g of powder was placed in a 20 mm graphite die and sintered in an SPS system (Dr. Sinter 1020). During sintering, the sample was: (i) first heated from room temperature to 600°C at a rate of 200°C/min, then (ii) heated from 600 to 900°C (the sintering temperature) at a rate of 50°C/min, (iii) held at 900°C for 5 min, and finally (iv) cooled to room temperature at a rate of 100°C/min. The maximum voltage and current were 4 V and 800 Amp, respectively. Sintering was performed under an applied uniaxial pressure was 60 MPa. A portion of this SPS $BaTiO_3$ pellet was heated to 1000°C for 6 hours for grain growth. For conventional sintering, green pellets (diameter 10 mm and thickness 2 mm) were made initially in a uniaxial press using a steel die and then isostatically pressed at a pressure of 225 MPa. The green pellets were then (i) heated from room temperature to the sintering temperature at a rate of 5°C/min, (ii) held at the sintering temperature for 120 min and (iii) finally cooled to room temperature at a rate of 5°C/min.

For samples sintered via pressureless sintering (PS), four different sintering temperatures (1200°C, 1225°C, 1250°C, 1275°C) were selected such that $BaTiO_3$ ceramics can be synthesized with comparable density but with different grain sizes. $BaTiO_3$ is known to undergo partial reduction when sintered in non-oxidizing atmosphere (e.g., vacuum) and/or at high temperature.[1,2] Additionally, the use of a graphite die in the SPS may cause diffusion of

carbon from the graphite die to the surfaces of the sintered materials and also result in reduction of $BaTiO_3$. Therefore, a post-sintering heat treatment procedure was employed (here after referred as air annealing) where all the sintered materials were further heated to 800°C and held for 6 hours in a tube furnace under an atmosphere of flowing oxygen (MTI Corporation, Richmond, California) to remove the carbon from the surfaces of the samples (sintered by SPS) and re-oxidize the $BaTiO_3$ grains. All the sintering and post-sintering heat treatment schemes are listed in **Table S1**.

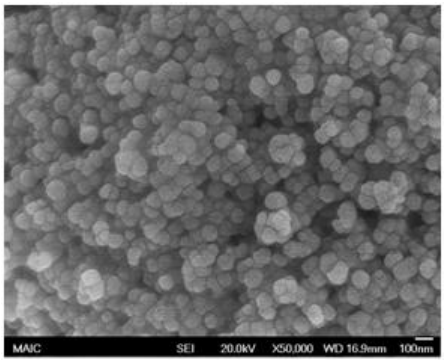

Figure S1. SEM micrograph of nanocrystalline $BaTiO_3$ powder.

Table S1: Sintering parameters and density measurements of $BaTiO_3$ ceramics by SPS and conventional sintering

Sintering technique	Sample ID	Sintering parameters			Annealing temp. (°C) and time (min)	Density g/cm^3 (%)
		Temp (°C)	Time (min)	Pressure (MPa)		
SPS	SPS_900	900	5	60	800, 360	5.7 (94.2)
	SPS_1000				1000, 360 and 800, 360	5.9 (98)
PS	PS_1200	1200	120	0	800, 360	5.7 (94.29)
	PS_1225	1225	120	0	800, 360	5.8 (97)
	PS_1250	1250	120	0	800, 360	5.8 (97)
	PS_1275	1275	120	0	800, 360	5.9 (97.6)

Microstructures

Microstructures of the sintered materials were imaged using scanning electron microscopy (SEM) (6335F FEG-SEM). Sintered $BaTiO_3$ specimens were first ground using 800 grit silicon carbide paper. The ground surfaces were next polished using a 0.5 μm alumina slurry and final polishing was done using a 0.04 μm colloidal silica slurry. Thermal etching was then used to reveal the microstructure on the polished surfaces. For the $BaTiO_3$ ceramics synthesized by SPS, no suitable thermal etching temperature was found. This is because thermal treatment could not exceed 900°C (the SPS sintering temperature) because grain growth would occur and thermal treatment below 900°C did not result any etching of the polished sample surfaces. For these materials, therefore, the average grain sizes were measured from the SEM micrographs of the fractured surfaces. For $BaTiO_3$ ceramics sintered at 1200°C and 1225°C by conventional sintering, thermal etching was performed at 1050°C for 1 hour whereas for $BaTiO_3$ ceramics sintered at 1250 and 1275°C, thermal etching was conducted at 1100°C for 1 hour. All the thermal etching treatments were conducted in a box furnace in air. As mentioned in the experimental section, the lineal intercept technique in accordance with the ASTM E112-10 standard was used to determine the average grain sizes of the sintered $BaTiO_3$ ceramics. **Figure S2** shows grain size distributions of all synthesized $BaTiO_3$ materials. All the conditions for thermal etching treatments and measured values of grain sizes are given in **Table S2**.

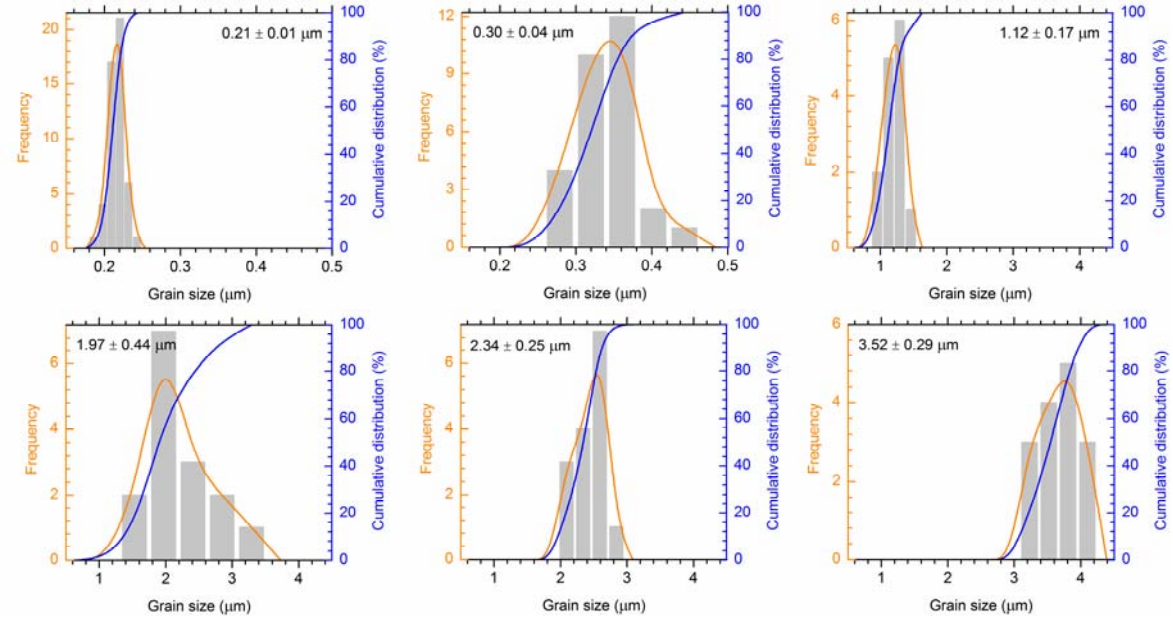

Figure S2: Grain size distributions of the synthesized $BaTiO_3$ ceramics.

Table S2: Thermal etching conditions, grain size, and relative permittivity (ε_r), dielectric loss ($\tan\delta$), and piezoelectric coefficient (d_{33})

Sample ID	Thermal etching parameters		Average GS (µm)	Dielectric properties (1 KHz)		d_{33} (*p*C/N)
	Temp (°C)	Time (min)		$\varepsilon_r/\tan\delta$ (RT)	$\varepsilon_r/\tan\delta$ (C_T)	
SPS_900	---	---	0.21 ± 0.01	3236/0.08 (32°C)	5161/0.09 (126.1°C)	138 ± 13
SPS_1000	---	---	0.30 ± 0.04	3424/0.04 (31.7°C)	9252/0.04 (130.7°C)	144 ± 14
PS_1200	1050	60	1.12 ± 0.17	4436/0.06 (31.9°C)	8305/0.04 (129°C)	160 ± 21
PS_1225	1050	60	1.97 ± 0.44	4841/0.03 (32°C)	10029/0.02 (129°C)	249 ±12
PS_1250	1100	60	2.34 ± 0.25	3798/0.02 (31.6°C)	7812/0.01 (129.5°C)	250 ± 7
PS_1275	1100	60	3.52 ± 0.29	3799/0.02 (31.6°C)	9145/0.03 (129.9°C)	247 ± 6

Specimen preparation for dielectric and piezoelectric

For dielectric and piezoelectric measurements, thin layers of gold (Au) were first deposited on two parallel surfaces of the annealed $BaTiO_3$ specimens via sputter deposition,

after which silver paste was applied on top of the Au. The silver paste was dried in air for 5 min. All dielectric and piezoelectric data measured on annealed $BaTiO_3$ samples are summarized in **Table S2**.

High-energy, in situ XRD measurements

For *in situ*, high-energy XRD measurements, smaller specimens of dimensions of 1 mm x 1 mm x 5 mm were cut from the larger sintered samples using a diamond saw, all the sides of the samples were polished, and samples were annealed at 300°C for 3 hours. Two of the parallel and opposing 1 mm x 5 mm surfaces of each sample were electroded using a silver paste.

All the XRD measurements were completed using an X-ray beam size of 0.2 mm x 0.2 mm and two-dimensional diffraction images were collected with a Perkin Elmer amorphous silicon area detector positioned in the forward direction (transmission geometry) at a distance of 2248 mm. A schematic of the experimental geometry and front view of the area detector image are shown in **Fig. S3**, where φ defines the azimuthal angle on the detector. At a value of φ=0°, the detector measures plane normals that are approximately parallel to the applied electric field and a value of φ = 90° corresponds to the perpendicular direction with to the applied electric field (Figure S2). From the two-dimensional diffraction images, segments of the ring patterns were integrated using the software package Fit2d[3] to obtain one-dimensional diffraction patterns. In the present work, ring patterns were integrated over an azimuthal angle of 15º (7.5º on each side of the direction parallel to the applied electric field).

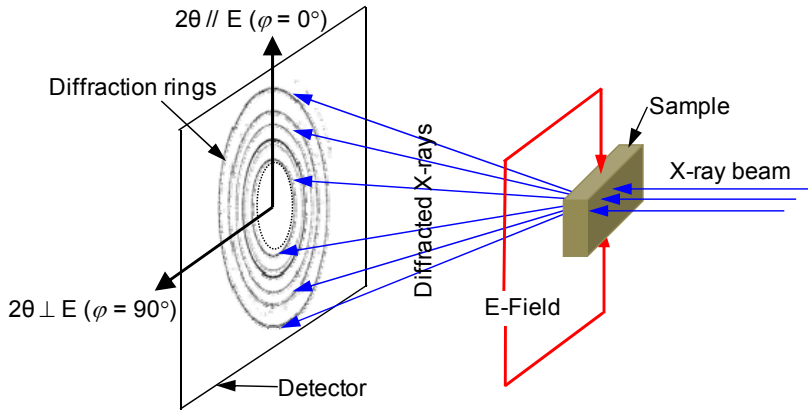

Figure S3: Schematic of experimental geometry and front view of detector image.

Determination of the extent of 90º domain reorientation

In tetragonal ferroelectrics, 90º domain wall motion can be observed and quantified from the changes in the changes in the volume fractions of the (002) and (200) orientation variants during electric field application. However, due to evolution of an additional phase during high electric field application in $BaTiO_3$, a new method was used that associates changes in the {002} diffraction profile with the macroscopic strain of the sample. For this purpose, a cumulative diffraction intensity distribution of interplanar spacing, *d*, across the {002} diffraction profile was used and the method has been described in the main text.

For the weak electric field measurements in which no field-induced secondary polymorph is observed, the 90º domain wall motion was calculated from the changes in the volume fractions of the (002) and (200) orientation variants. In perovskite ferroelectrics with a tetragonal crystal structure, the volume fraction of the material with (002) domains parallel to a particular direction of specimen is given by:[4]

$$v_{002} = \frac{\frac{I_{002}}{I'_{002}}}{\frac{I_{002}}{I'_{002}} + 2\left(\frac{I_{200}}{I'_{200}}\right)} \qquad \text{(S.1)}$$

where I_{hkl} is the integrated area of the *(hkl)* Bragg peak for a given sample with a preferred orientation of 90º domains and I'_{hkl} is the integrated area of the same Bragg peak for a sample where 90º domains have no preferred orientations.[4] In a sample with random orientation of 90º domains, the value of v_{002} is equal to 1/3. Therefore, during electric field application, the volume fraction of the (002) domains (η_{002}) that has been reoriented in the direction of the applied field is given by[4]

$$\eta_{002} = v_{002} - \frac{1}{3} \ . \tag{S.2}$$

If η^{+}_{002} and η^{-}_{002} represent the volume fractions of the 002 domains oriented in a particular direction during the positive and negative electric field cycles (bipolar electric field for subcoercive measurements) respectively, then the volume fraction of the (002) domains that are reoriented in a specific sample direction ($\Delta\eta_{002}$) is expressed relative to the maximum and minimum values through,[5]

$$\Delta\eta_{002} = \eta^{+}_{002} - \eta^{-}_{002} \ . \tag{S.3}$$

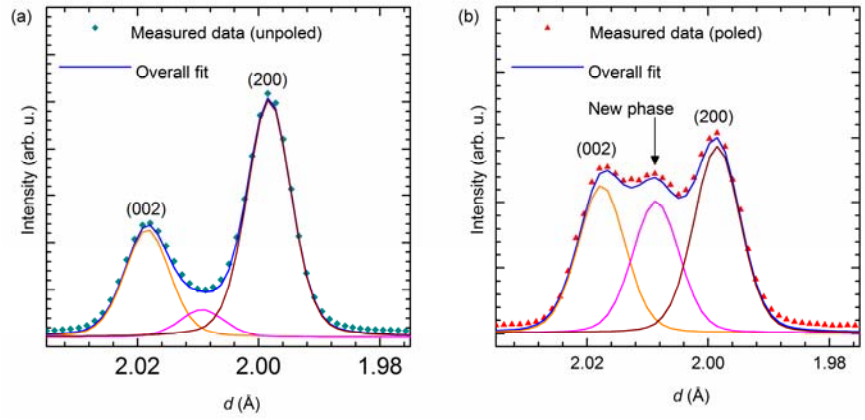

Figure S4: Representative fit of {200} reflections measured (a) prior electric field application and (b) during electric field application for the sample with a grain size of 3.52 µm using three symmetric pseudo-Voigt profile functions.

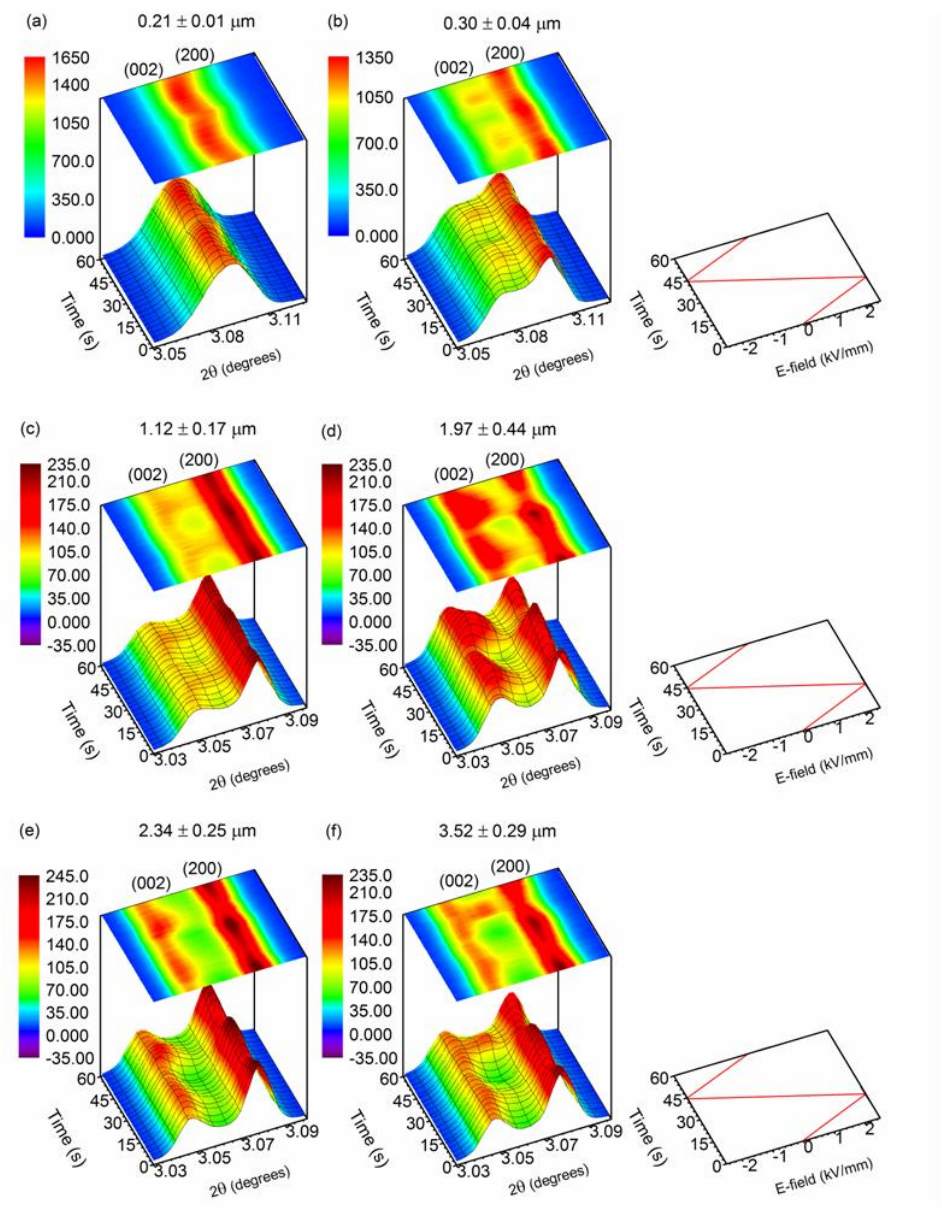

Figure S5: Contour plots of changes in intensities of {002} diffraction profile containing the (002) and (200) tetragonal phase reflections during electric field application (±2.5 kV/mm), revealing variation in extent of domain wall motion in various grain size $BaTiO_3$ ceramics.

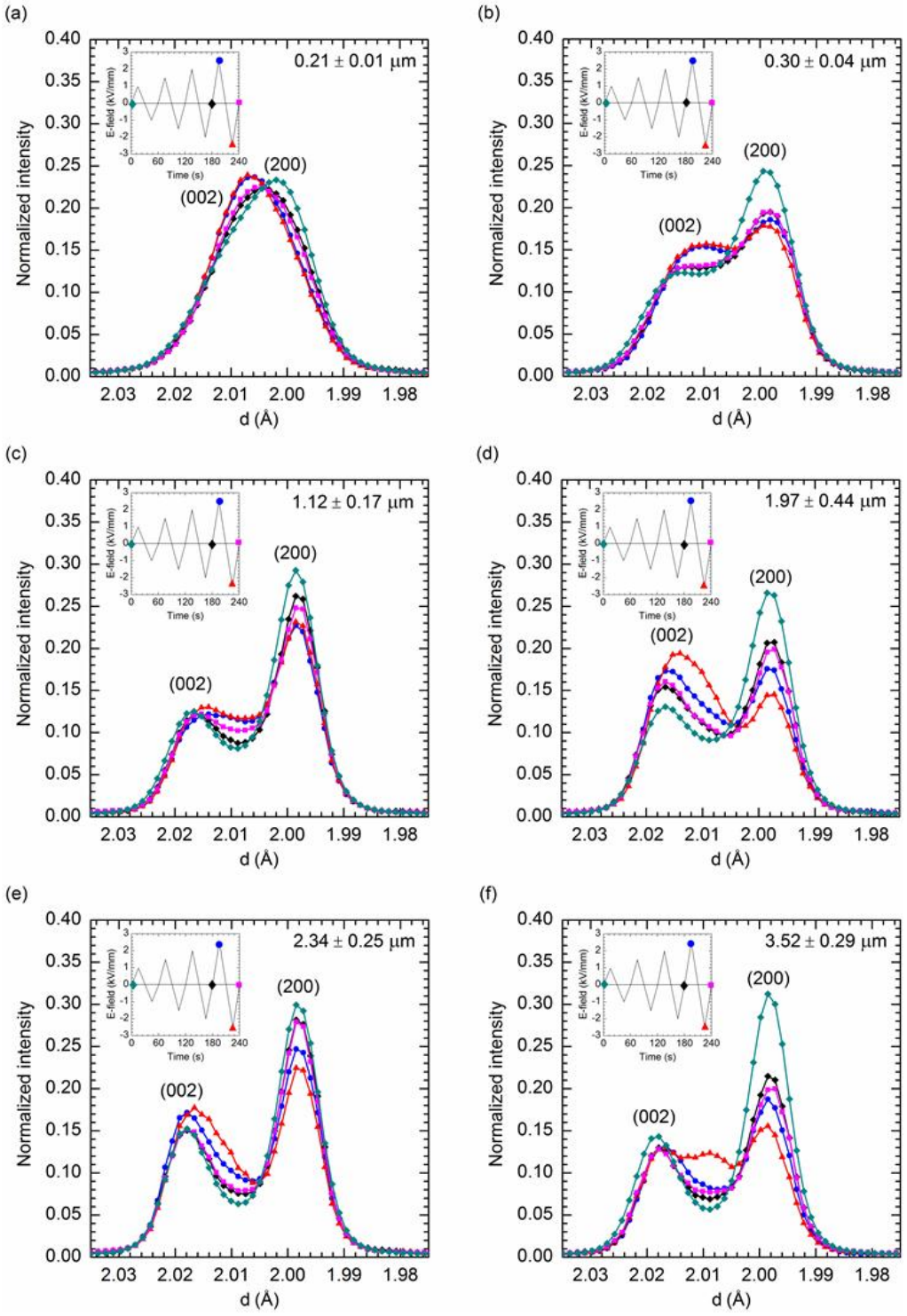

Figure S6: Selective XRD patterns measured prior and during electric field application (± 2.5 kV/mm) for all the grain sizes of $BaTiO_3$.

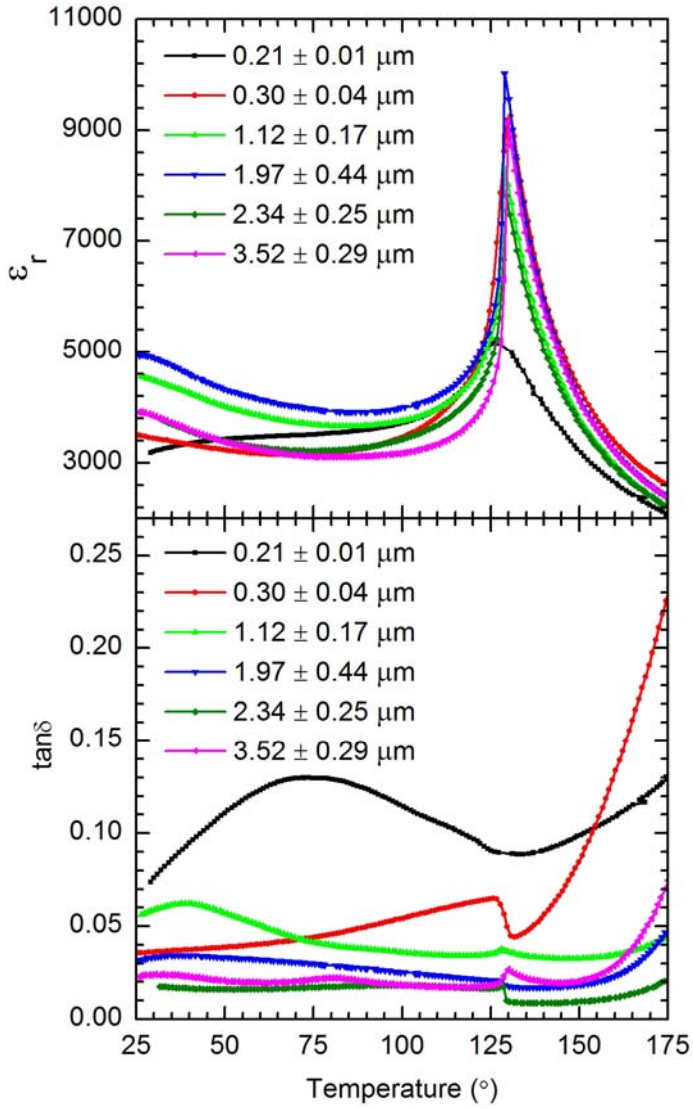

Figure S7: Dielectric permittivity and loss of the $BaTiO_3$ samples of different grain sizes as a function of temperature at 1 kHz.

References

[1] Ghosh, D., Han, H., Nino, J. C., Subhash, G., & Jones, J. L. Synthesis of $BaTiO_3$-20wt%$CoFe_2O_4$ nanocomposites via spark plasma sintering, *J. Am. Ceram. Soc*. **2012**, *95*, 2504.

[2] Yoon, S. et al. Spark plasma sintering of nanocrystalline $BaTiO_3$- powders: consolidation behavior and dielectric characteristics, J. Eur. Ceram. Soc. **2011**, *31*, 1723.

[3] Hammersley, A. P. Fit2D. 1987, ESRF: Grenoble, France (fit2d_12_077_i686_WXP).

[4] Pramanick, A., Damjanovic, D., Daniels, J. E., Nino, J. C. & Jones, J. L. Origins of electro-mechanical coupling in polycrystalline ferroelectrics during subcoercive electrical loading, J. Am. Ceram. Soc. **2011**, *94*, 293.

[5] Seshadri, S. B. Prewitt, A. D. Studer, A. J. Damjanovic, D. & Jones, J. L. An in situ diffraction study of domain wall motion contributions to the frequency dispersion of the piezoelectric coefficient in lead zirconate titanate, Appl. Phys. Letts. **2013**, *102*, 042911.